Patterns of Nuclear Magnetic Shielding of Transition-Metal Nuclei

JOAN MASON

Department of Chemistry, The Open University, Milton Keynes MK7 6AA, U.K.

Received November 14, 1986 (Revised Manuscript Received May 4, 1987)

Contents

I. Introduction 1299
II. Practical Limitations to Transition-Metal NMR Spectroscopy 1300
III. Periodicity of the Ranges of Chemical Shifts of the Elements 1301
IV. Periodicity of the Radial Parameters 1301
V. Factors in Nuclear Magnetic Shielding 1302
VI. Comparison of the Periodicities for Transition and Main-Group Elements 1302
A. Effects of Local Symmetry 1302
B. Irregularities in the Periodicity 1303
VII. Other Measures of Shielding Sensitivity 1303
VIII. Spectrochemical and Nephelauxetic Effects of the Ligands 1304
A. The Spectrochemical Series 1304
B. The Nephelauxetic Series 1304
C. Quantification of Spectrochemical and Nephelauxetic Effects 1304
D. Periodicities in Chemical Shift Additivities 1305
E. Periodicities in Spectrochemical and Nephelauxetic Effects of the Metal 1306
F. Early and Late Transition Elements 1306
IX. Solid-State Studies 1307
X. Dependence of the Shielding on Metal Oxidation State and M–M Bond Order 1310
XI. Relativistic Effects in Transition-Metal Shielding 1311
XII. Conclusions 1311
XIII. References 1311

Joan Mason received her degrees (B.A., MA., Ph.D., and Sc.D.) from Cambridge University and is now a Reader in Chemistry at The Open University. She has worked in boron and fluorine chemistry with H. J. Emeléus, in boron chemistry with A. B. Burg at the University of Southern California, and in nitrogen, sulfur, molybdenum chemistry, etc., at University College, London, University of East Anglia, and The Open University since 1970, with time out to raise three children. Current research interests include NMR spectroscopy, the interpretation of NMR parameters (including shielding tensors), particularly of transition-metal and ^{15}N nuclei, and bio-NMR.

I. Introduction

Advances in multinuclear NMR spectroscopy have now provided a large but diffuse data base of NMR parameters for transition-metal nuclei.[1-14] This review examines regularities in their coordination shifts in inorganic and organometallic complexes. Commonly, nuclear magnetic shielding is studied for a particular metal or periodic group in isolation, but this phenomenon is a complex one, as two or more factors are influential and their effects are not easy to separate. As ever, further insight may be gained from the periodic relationships,[15,16] and the generalizations that emerge have practical value as well as chemical interest.

Over the decades, links have been made between transition-metal nucleus shielding and results from electronic spectroscopy, particularly ligand field splittings and nephelauxetism (≡cloud expansion) of the d electrons. Here, too, there are important periodicities that can help to disentangle the causative factors. Reciprocally, it should be possible to complement the optical spectroscopic information with conclusions from the metal nucleus shielding in complexes with (formal) d^0 or d^{10} configurations, or with ligand field absorption obscured by stronger bands.

An additional purpose of this review is to further the development of a physical picture for the understanding of NMR shifts. Chemists have a mechanical image for vibrational spectroscopy, and even for one-electron "jumps" in electronic and electron spectroscopy. Such a picture began to develop in the form "the more negative the charge density, the higher the shielding", but this generalization is well-known to be unreliable. Indeed, the deshielding with increase in electronegativity of substituents is part of a periodic relationship that holds across the row of the substituent and is reversed down the group.[16] A physical picture is, however, possible, in terms of paramagnetic circulations in the valence shell, deshielding the resonant nucleus. Such a picture derives from the second-order perturbation theory;[17] the chemical shift arises from the mixing in by the magnetic field of excited states that are magnetic dipole allowed and so involve electronic circulations or currents that reinforce the applied field.

For compounds of the transition metals, therefore, a major role is played by d–d (i.e., $d\pi \rightarrow d\sigma^*$) circula-

0009-2665/87/0787-1299$06.50/0

TABLE I. NMR Properties of the Transition Metals (Most Favorable Nucleus Listed in Each Case)

	^{45}Sc	^{49}Ti	^{51}V	^{53}Cr	^{55}Mn	^{57}Fe	^{59}Co	^{61}Ni	^{63}Cu	^{67}Zn
I	$^7/_2$	$^7/_2$	$^7/_2$	$^3/_2$	$^5/_2$	$^1/_2$	$^7/_2$	$^3/_2$	$^3/_2$	$^5/_2$
NA, %	100	5.51	99.76	9.55	100	2.19	100	1.19	69.09	4.11
$R^{c\,a}$	1720	1.18	2170	0.485	1014	0.0042	1560	0.242	368	0.671
Q, 10^{-28} m^2	−0.22	0.24	0.052	−0.15	0.40		0.42	0.16	−0.22	0.15
	^{89}Y	^{91}Zr	^{93}Nb	^{95}Mo	^{99}Tc	^{99}Ru	^{103}Rh	^{105}Pd	^{109}Ag	^{113}Cd
I	$^1/_2$	$^5/_2$	$^9/_2$	$^5/_2$	$^9/_2$	$^5/_2$	$^1/_2$	$^5/_2$	$^1/_2$	$^1/_2$
NA, %	100	11.23	100	15.72		12.72	100	22.23	48.18	12.26
R^c	0.676	6.05	2770	2.92		0.815	0.180	1.43	0.280	7.69
Q, 10^{-28} m^2		−0.21	−0.32	−0.015	−0.13	0.076		0.6		
	^{175}Lu	^{177}Hf	^{181}Ta	^{183}W	^{187}Re	^{187}Os	^{193}Ir	^{195}Pt	^{197}Au	^{199}Hg
I	$^7/_2$	$^7/_2$	$^7/_2$	$^1/_2$	$^5/_2$	$^1/_2$	$^3/_2$	$^1/_2$	$^3/_2$	$^1/_2$
NA, %	97.41	18.50	99.9	14.28	62.93	1.64	62.7	33.8	100	16.84
R^c	173	1.47	213	0.061	511	0.0011	0.12	19.9	0.15	5.68
Q, 10^{-28} m^2	3.46	3.3	3.3		2.2		0.78		0.55	

	^{139}La	^{171}Yb	^{235}U		^{139}La	^{171}Yb	^{235}U
I	$^7/_2$	$^1/_2$	$^7/_2$	R^c	343	4.5	0.0054
NA, %	99.9	14.31	0.72	Q, 10^{-28} m^2	0.22		4.55

[a] R^c is the receptivity relative to that of ^{13}C in natural abundance.

tions. The deshielding is more effective the lower the excitation energy (a spectrochemical dependence), the closer the circulation to the resonant nucleus (a nephelauxetic dependence), and the larger the angular imbalance of charge in the valence shell, producing the orbital angular momentum that is unquenched by the magnetic field.[15-17]

Nuclear magnetic shielding is of course a tensor property, since the electronic circulations use orbitals related to the bond axes. In an anisotropic molecule, therefore, the shielding differs according to the direction of the magnetic field relative to the molecular axes, but only the averaged shielding is observed in the liquid phase. The individual tensor elements can, in principle, be measured in the solid state.[18,19] Unfortunately, as discussed in section IX, relatively few measurements have so far been possible for transition-metal nuclei, in contrast to lighter nuclei with more favorable NMR properties, and general discussions of ligand field effects rely substantially on comparisons of complexes of the same symmetry and electron configuration, without mixed ligands (whether d^0, d^2, d^4, d^6, d^8, or d^{10}).

The development of transition-metal NMR spectroscopy has been very uneven because of the very small number of nuclei with favorable nuclear properties for high-resolution NMR. But as the technology evolves, more nuclei and bond types, and also the solid state, are being brought into the spectroscopist's net. The literature is now so large that reference must be made in general to the reviews[1-14] rather than to individual papers.

II. Practical Limitations to Transition-Metal NMR Spectroscopy

NMR properties of the transition-metal nuclei are given in Table I. Favorable properties for high-resolution NMR are spin quantum number $I = {}^1/_2$, or for $I > {}^1/_2$ a relatively small value of the nuclear electric quadrupole moment eQ and a larger value of I, to minimize quadrupolar broadening, as discussed below. Also necessary are a sufficiently large natural abundance (A) and magnetogyric ratio γ (effectively the ratio of the magnetic moment to the spin quantum number), to which the NMR frequency is proportional. The intrinsic NMR receptivity, which is a measure of the intensity of signal to be expected, increases as $|\gamma^3|AI(I+1)$. Thus, larger values of I are more favorable, by a factor of 33 from $I = {}^1/_2$ to $I = {}^9/_2$. Transition-metal nuclei with natural abundance below 5% that may usefully be studied with enrichment are ^{57}Fe, ^{61}Ni, ^{67}Zn, and ^{187}Os.

Spin $^1/_2$ nuclei with low γ values have a further problem of too slow relaxation, since the rate depends on γ, and long accumulation times or sensitivity enhancement techniques may be needed for adequate sensitivity: examples are ^{89}Y, ^{183}W, ^{57}Fe, ^{187}Os, ^{103}Rh, and ^{109}Ag.

The majority of transition-metal nuclei have $I > {}^1/_2$ and therefore a quadrupolar disposition of electric charge. The electric quadrupole is coupled to the spin (magnetic dipole), since transitions in the one change the magnetic environment of the other. Whereas the orientation of the spin dipole is quantized relative to the magnetic field, that of the electric quadrupole is quantized relative to the electric field gradient (efg) eq at the nucleus due to the electrons and the other nuclei; the nuclear electric quadrupole coupling constant (NQCC) is $\chi = e^2qQ/h$ (in frequency units). The nuclear energy levels therefore depend on both the efg and the magnetic field. In the liquid phase rapid and isotropic molecular tumbling averages the quadrupolar (as well as the dipolar) interactions; but the relaxation of the electric quadrupole with fluctuations of the efg (e.g. in molecular collisions) relaxes the nuclear spin also, and fast relaxation leads to uncertainty over the line position, i.e. *quadrupolar broadening*. The quadrupolar relaxation rate and the line width are proportional to $\chi^2(1 + \eta^2/3)(2I + 3)/I^2(2I - 1)$ (where η is the asymmetry parameter of the efg, maximally equal to 1, and 0 for axial symmetry) and also to the correlation time τ_c, where $(\tau_c)^{-1}$ is (e.g.) the rate of molecular tumbling. The quadrupolar broadening therefore increases sharply with increase in Q and in the efg q. Again, higher values of I are advantageous because of the line width dependence on $(2I + 3)/I^2(2I - 1)$, which decreases by a factor of 67.5 from $I = 1$ to $I = {}^9/_2$.

For a given nucleus line widths are minimized for small molecules in low-viscosity samples (τ small), with highly symmetry environments of the metal nucleus (q

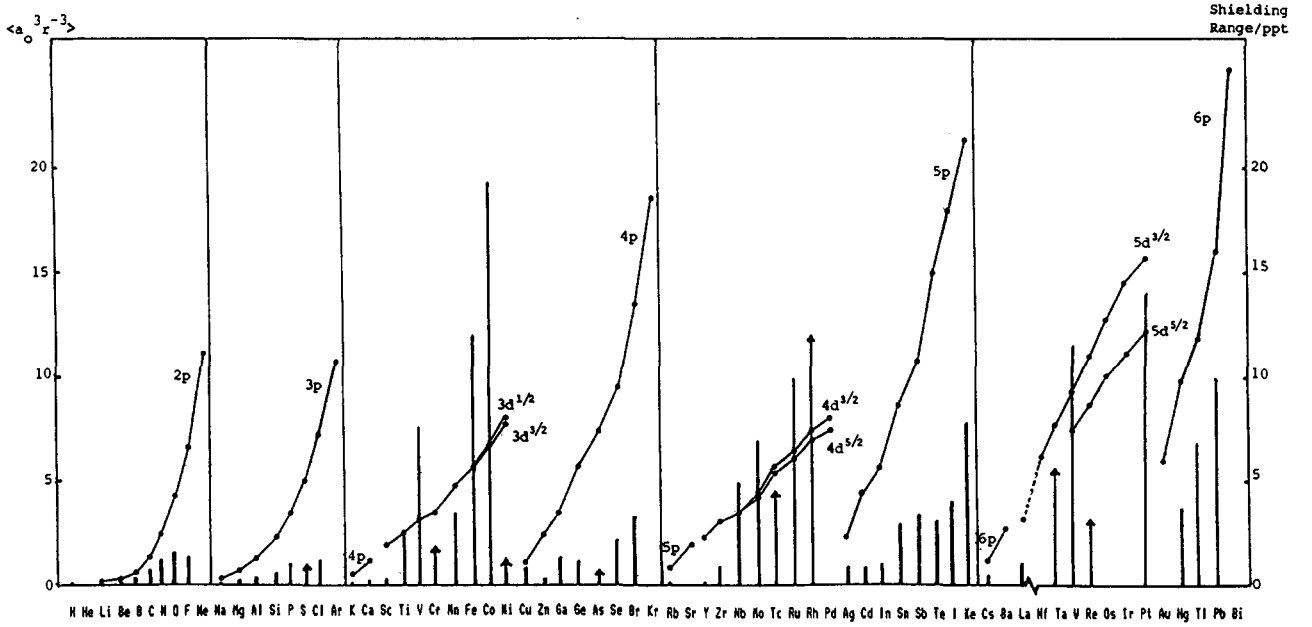

Figure 1. Comparison of the periodicity of the nuclear magnetic shielding ranges (in parts per thousand) with that of the p, d valence electron radial functions for the free atoms. The derivation of the values is given in the text. r is in units of a_0, the Bohr radius, which is equal to 52.9 pm. The ranges cover diamagnetic compounds only and exclude metallic compounds showing Knight shifts. Arrows indicate ranges that are limited by unfavorable nuclear properties.

small). Examples are tetraoxo $[MO_4]^q$ or fully fluorinated species $[MF_6]^q$, or perhaps $M(CO)_6$, and for some quadrupolar metal nuclei these are the only types of compounds for which an NMR signal has been reported. (In partially fluorinated species the efg and line width may be large because of differing electronegativities of the substituents.) As an example of heroic measures, a signal 20 kHz in width was raised for ^{235}U in liquid UF_6 at 380 K (viscosity low), with 130-fold enrichment (to 93.5%).[20] Transition-metal nuclei for which NMR spectroscopic studies have not as yet been reported are ^{175}Lu, ^{177}Hf, ^{105}Pd, ^{189}Os, ^{193}Ir, ^{197}Au, also ^{235}U (more than one signal being needed!). Nuclei giving inconveniently broad lines include ^{181}Ta, ^{53}Cr, and ^{99}Re.

For certain metals NMR study has been limited by a restricted range of diamagnetic compounds, as for Cu and Ag in solution, lanthanides, and actinides. Table I includes only those lanthanides giving diamagnetic compounds, though not cerium as this has no sufficiently stable magnetic nucleus.

III. Periodicity of the Ranges of Chemical Shifts of the Elements

A periodicity in the observed ranges of chemical shifts for diamagnetic compounds, as noted over 20 years ago for the main-group elements,[21] is now evident in the transition series also, as shown in Figure 1. The shift range has practical value as a measure of the shielding sensitivity. This is important for the transition elements, since the majority of them have no stable nuclide with spin $^1/_2$ and quadrupolar broadening is more tolerable with a greater shift dispersion. Further, the theoretical interpretation of the periodicity offers clues as to important determinants of the shielding.

Figure 1 shows that in the transition series, the shift ranges are small to the left of the periodic table and increase across the row. The picture is incomplete, particularly in the third series, but some key relationships are unmistakable: thus, ^{51}V is now a well-studied nucleus, but the shift range for vanadium compounds is clearly less than half that for cobalt compounds, although the ranges of bond types are not very different for the two elements. (The range for ^{55}Mn is limited by the range of diamagnetic compounds.) Similar comparisons can be made in the second and third transition series. For the main-group elements the shift ranges increase down the group, except that those for the second row (lithium to fluoride) are larger than those for the third. Certain of these group trends are echoed in the transition series, as will be discussed.

IV. Periodicity of the Radial Parameters

The periodicity of shift ranges of the main-group elements was related[21] to that of the inverse cube of the valence p-electron radius $\langle r^{-3} \rangle_p$, as obtained[22] from spin–orbit splittings in atomic spectra.[23] The $\langle r^{-3} \rangle_p$ values in Figure 1 were so determined, and the corresponding values of $\langle r^{-3} \rangle_d$ for valence [i.e. $(n - 1)$d] electrons were calculated from relativistic Hartree–Fock–Slater atomic wave functions.[24] The inverse cube is the distance dependence for dipolar interactions, and therefore the radial dependence of the paramagnetic term in the Ramsey shielding theory,[17] the origin being taken at the resonant nucleus. The periodicity of this radial term is related to that of Z_A^3, where $Z_A e$ is the effective nuclear charge as experienced by a valence electron.[25] The radial term increases across the row of the main-group elements, or across a transition series, because of incomplete screening by electrons in the same shell and interelectron repulsion. It increases down the group also, as the valence p or d orbitals become more penetrating though more diffuse. This periodicity has well-known irregularities, due to the irregular buildup of the shells, such as those observed for the posttransition elements.[26,27]

The time spent by the valence electron close to the nucleus is important to nuclear magnetic shielding. The larger ranges of the radial term for main-group than for

transition elements of the same principal quantum number, as evident in Figure 1, relate to the greater penetration of p than d electrons.

For purposes of comparison, free-atom values for the radial term are plotted in Figure 1. The value for an atom in a molecule is of course modified by effects of substituents and overall charge, from which nephelauxetic effects may be separated out, as discussed below.

V. Factors in Nuclear Magnetic Shielding

A ligand field "atom in a molecule" formulation[28] of the second-order perturbation theory[17] gave the paramagnetic term σ_p as in eq 1, summing over the d-elec-

$$-\sigma_p = (\mu_0/4\pi)(e^2/m^2)(\Delta E)^{-1}\langle r^{-3}\rangle_d\langle 0|L^2|0\rangle \quad (1)$$

tron excitations in a d^6 octahedral complex, and corresponding formulas were developed for square-planar[29] and other geometries. The paramagnetic term largely determines the chemical shift δ (although σ and δ are, unfortunately, defined with opposite signs). The paramagnetic term is balanced by a first-order (diamagnetic) term σ_d, the variation of which is much smaller and can be neglected in qualitative discussions.[16] The magnitudes of σ_d and σ_p depend on the choice of gauge origin, which is conveniently located at the resonant nucleus.

There is a voluminous literature,[15,30] reviewed annually,[31] of theoretical calculations of nuclear magnetic shielding, by ab initio and semiempirical methods. Relative little attention has been paid as yet to the transition elements because of the computational problems. A good start at the ab initio level has, however, been made by Nakatsuji and co-workers, who report calculations for manganese shielding in representative d^6 complexes,[32] and for silver, cadmium, copper, and zinc in representative d^{10} complexes.[33] Their results will be mentioned in context in sections VIII and IX, and their papers afford a good demonstration of the articulation of the shielding theory, since they contain detailed tabulations of the contributions calculated.

Equation 1 shows that the deshielding is greater the closer is the paramagnetic circulation to the resonant nucleus (r small), the smaller the frontier orbital gap for magnetically active excitation (ΔE small), and the greater the angular imbalance of charge ($\langle 0|L^2|0\rangle$ large). This is zero for closed shells, as in free ions, or core electrons. The angular and radial functions are usefully discussed separately.

In transition-metal compounds r is normally the valence d-electron radius and ΔE the ligand field splitting Δ, or a weighted mean of the splittings for lower symmetries. (Valence shall p contributions become important only toward the end of the transition series, as demonstrated by Nakatsuji et al.[32,33] and discussed further below.) The shielding therefore increases (for a given d-electron configuration) with increase in the ligand field strength, following the spectrochemical series, and also with increase in delocalization, decreasing the radial factor $\langle r^{-3}\rangle_d$.[28]

This expansion of the d shell is an intricate question. It is manifest as a decrease of optical parameters from the free metal ion to the complex, arising from decrease in interelectron (Coulomb) repulsion because of delocalization of the charge.[26,34-36] It has been described in terms of L–M covalency, π back-bonding or antibonding, σ antibonding, polarizability, the electroneutrality principle, L $\leftrightarrow$ M charge transfer, spin delocalization, and so on, effects that are difficult to separate experimentally. There are some operational definitions, e.g. of an "orbital reduction factor" (in fact a reduction factor allowing for the d-orbital expansion in the complex)[34] k' or $k_{\sigma\pi}$, defined as unity for pure d orbitals, which is somewhat reduced in the first transition series and further reduced in the second and third.[35] A useful description is in terms of nephelauxetism, defined by optical (Racah) parameters of interelectron repulsion.[36] A comparable parameter can be obtained from the reduction in spin–orbit coupling in the complex compared to the free ion.[37]

In formulations of the paramagnetic term the radial function has been expressed as $k'\langle r^{-3}\rangle_d$,[38] or else a nephelauxetic parameter may be incorporated,[39] as described below. Alternatively, calculated coefficients have been used; thus, the radial dependence may be expressed as $(C_M)^2\langle r^{-3}\rangle_d$, where C_M is the coefficient of the d(M) orbital in the LCAO description of the MO.[40] Similarly, $\langle r^{-3}\rangle_d$ may be reduced in proportion to a calculated reduction of the central charge by L $\rightarrow$ M charge transfer, as in metalate ions.[41]

For main-group elements a radial term dependence is evident also in many of the shielding patterns that are observed. Examples are the correlations of carbon shifts with electron density in aromatic systems, or with σ-inductive effects. An increase in positive atomic charge, as with electronegative substituents, contracts the valence orbitals and decreases the shielding; cf. the effects of nephelauxetic type observed in resonance of ^{27}Al or ^{199}Hg.[42] Dependence of the energy term is evident when there are particularly low-lying magnetic dipole allowed excited states, as in nitrogen shifts in groups with low-energy $n(N) \rightarrow \pi^*$ circulations.[43]

VI. Comparison of the Periodicities for Transition and Main-Group Elements

A. Effects of Local Symmetry

Figure 1 clearly shows that the shift ranges are much larger for transition elements than for main-group elements of similar principal quantum number, despite smaller $\langle r^{-3}\rangle_d$ than $\langle r^{-3}\rangle_p$ values later in the series. The greater shift ranges are no doubt related to the larger range of $\langle 0|L^2|0\rangle$ values for valence orbitals of higher angular momentum quantum number. Some shielding formulations contain explicit terms (normally derived from orbital populations) such as $\sum Q$ in eq 2[25] or P_i and D_i in eq 3[21] to express the imbalance of charge in the valence p and d shells, where ΔE is a mean or effective excitation energy.

$$-\sigma_p = (\mu_0/4\pi)2\mu_B^2(\Delta E)^{-1}\langle r^{-3}\rangle_p\sum Q \quad (2)$$

$$-\sigma_p = (2\mu_0/3\pi)\mu_B^2(\Delta E)^{-1}[\langle r^{-3}\rangle_p P_1 + \langle r^{-3}\rangle_d D_i] \quad (3)$$

For main-group elements variations due to changes in local symmetry are relatively small. In singly bonded compounds the $\sum Q$ term in eq 2 takes values from 2 for carbon or nitrogen, reducing to $^5/_3$ for oxygen and 1 for fluorine (cf. 0 for a free atom or ion). $\sum Q = 2$ also for triply bonded carbon or nitrogen, because of zero

TABLE II. Chemical Shifts (δ) of Transition-Metal Nuclei in d^0 Tetraoxo Species Relative to Those in the Corresponding d^6 Hexacarbonyls

	$\delta[MO_4^{3-}] - \delta[M(CO)_6^-]$		$\delta[MO_4^{2-}] - \delta[M(CO)_6]$		$\delta[MO_4^-] - \delta[M(CO)_6^+]$
V	1415	Cr	1800	Mn	1445
Nb	1200[a]	Mo	1857		
Ta	≈1900	W	3500	Re	3400

[a] Based on an extrapolated value for $\delta(NbO_4^{3-})$.

orbital angular momentum about the linear axis. It is maximal in planar groups, increasing to 2.5–2.8, depending on substituents.[25] In eq 3, the d-electron contribution is usually unimportant for main-group elements and P_i takes values from 0 (for spherical symmetry) to 2, for two p orbitals filled and one empty (or vice versa), again depending on the element and the bonding. Variations in ΔE are not much greater than this and are comparable for different bond types of the same element, and for different elements. Hence, the dominance of the radial term in the periodicity of the shift ranges of main-group elements.[21]

For transition elements, however, the D_1 parameter in eq 2 can take values up to 12, for three of the d orbitals filled and two empty (as in low-spin d^6 octahedral complexes) or vice versa (e.g., d^4 tetrahedral). Of the remarkable range of over 19 000 ppm of ^{59}Co shifts more than 16 000 ppm are spanned by octahedral Co(III) complexes, with the lower oxidation states contributing overlapping ranges to lower frequencies. Thus, the larger angular momentum integrals amplify the differences in substituent effects, which themselves may be greater in transition-metal than in main-group compounds. In discussions of spectrochemical and nephelauxetic effects it is necessary to avoid or minimize variation in the angular terms, by considering only compounds of similar symmetry and d-electron configuration.

Closer examination of the shift ranges in Figure 1 shows effects of the different chemistry of different groups or rows, such as a diversity of bond types for particular elements increasing the variation in angular imbalance and in ΔE, and therefore the range of chemical shift. A factor limiting the ranges for groups 1, 2, and 7 is, no doubt, the paucity of bond types, and this is evident in the smaller range observed for fluorine than for oxygen shifts.[21] Similarly the ranges for the scandium, copper, and zinc groups are limited by the small number of accessible oxidation states.

B. Irregularities in the Periodicity

A pleasing anomaly in the periodicity in Figure 1 is the dip in shielding ranges at the third row (Na to Cl) in Figure 1, although the $\langle r^{-3}\rangle_{np}$ values are rather similar for corresponding elements in the second and third rows: in fact the $\langle r^{-3}\rangle_p$ values for the second-row elements are anomalously large compared to those for later rows. These properties can be linked with the anomalous chemistry of the first member of a main group (e.g., C, N, O, and F) compared with that of subsequent members (Si, P, S, Cl, etc.).[26,27] Second-row atoms are distinctive in their octet restriction, and also their relatively high electronegativity, small atomic size, and tendency to form multiple bonds. Many "second-row anomalies" have a common origin in the small number of inner electrons, only two, for these atoms. This enhances the valence electron penetration, and also (because of the small atomic size) the $p\pi$ overlap, or repulsion of lone pairs on adjacent atoms. Thus, N–N, O–O, and F–F bonds are long and weak (ΔE small), and CO_2, N_2, and nitrogen oxides are multiply bonded, whereas SiO_2, P_n, and oxides of phosphorus are singly bonded (ΔE large). The greater shift ranges for the second-row elements thus reflect the magnitude of the radial factors, and also the greater range of angular imbalance and of ΔE (with the inclusion of low-energy $n \rightarrow \pi$ and $\sigma \leftrightarrow \pi$ circulations).

The radial terms $\langle r^{-3}\rangle_d$ are similar for the first and second transition series, echoing the similarity for the second and third rows of the table: that is, they are "enlarged" in the first transition series because of the small number of inner electrons. They are greatly increased in the third transition series, as in the sixth row of the table, because of the filling of the f shell (the lanthanide contraction) and relativistic effects. In the heavier elements, it is likely that the shift ranges are extended by spin–orbit coupling and other relativistic effects (as discussed in section XI) and by the availability of d,f orbitals. Interestingly, one of the largest observed ranges for a main-group element is that of nearly 8000 ppm for the noble gas xenon, from the free atom to XeO_6^{4-}.

Despite the gaps in the record so far, some trends down the transition groups are emerging. Shielding ranges in the first transition series are large compared to those in the second, as for the second relative to the third row of the main-group elements, reflecting important differences in the bonding in the first series. That the shift ranges are comparable in the first and third transition series may be related to a large range of ΔE values in the first series, as discussed in section VIII.

VII. Other Measures of Shielding Sensitivity

For comparisons to include elements with less favorable nuclear properties other approximate measures of shielding range can be used, such as the difference in chemical shift between highly symmetric species for which quadrupolar nuclei give narrower lines. Values of the chemical shift in the d^0 tetraoxo compound relative to that in the d^6 hexacarbonyl are given in Table II, and some shifts for halide complexes, in Table III.

TABLE III. Chemical Shifts (δ) of Transition-Metal Nuclei in d^0 or d^6 Hexachloro Complexes Relative to Those in the Corresponding Hexafluoro Complexes

$[MX_6^{2-}]$, d^0		$[MX_6^-]$, d^0		$[MX_6]$, d^0		$[MX_6^{3-}]$, d^6		$[MX_6^{2-}]$, d^6	
Ti	≈900[a] (≈280)[c]	V	≈1100[b]						
Zr	792	Nb	1550			Rh	(−900)[c]		
		Ta		W	3300			Pt	−7300 (−1900)[c]

[a] Based on an extrapolated value for $[TiCl_6^{2-}]$. [b] Estimated from $\delta[VOCl_4^-] - \delta[VOF_4^-] = 820$ ppm. [c] Shift from the hexabromo to the corresponding hexachloro complex.

These comparisons indicate rather similar values in the first and second transition series, and larger values in the third. Shift ranges for tungsten are greater than for molybdenum;[44] but the ranges for rhodium and platinum are contracted relative to those for cobalt and probably iron.

These differences from the trends in the main groups are usefully discussed in terms of substituent effects, which can be labeled for convenience as "spectrochemical" effects involving the energy term ΔE, and nephelauxetic effects on the radial term $\langle r^{-3} \rangle_d$, as related to delocalization and covalency.

VIII. Spectrochemical and Nephelauxetic Effects of the Ligands

A. The Spectrochemical Series

Since the first reports in cobalt resonance,[28,45] there have been many δ/λ correlations of transition-metal shifts δ with the inverse energy or wavelength λ of the longest wavelength spin-allowed d–d transition; for Co(III), λ varies over the range 300–750 nm. The metal shielding might then be expected to follow the spectrochemical series of increase in ligand field splitting Δ. This well-studied series can be written approximately as a sequence of ligating atoms: I < Br < Cl < S < F < O < N < C < H.[31] The ordering resembles that of decrease in atomic radius, i.e. of closer approach of the ligands, or stronger bonding. Synergic ($\sigma + \pi$) bonding increases Δ, so that Se < S < O, but As $\simeq$ P > N in this series.[26]

Indeed, complexes of strong ligands such as Cp, CO, PF_3, and H show high metal shielding, and the shielding sequence F < O < N < C is observed. For ligating atoms lower in the periodic groups, however, the δ/λ plot gives lines of decreasing slope; in cobalt resonance the slope is almost halved from second- to third-row ligands. The increase in shielding in the sequence Cl < Br < I was attributed to increase in the d-electron radius with increase in polarizability of the ligand down the group, and the connection was made[34,35] with the nephelauxetic series of the ligands.[31] Platinum shifts with changes in halide ligands were related to changes in M–L covalency and the metal radial function,[36] and similarly for other transition metals.[1-16]

Complexes that clearly show the spectrochemical sequence of increase in the metal shielding as I < Br < Cl < F are those of formally d^0 transition metals with halide or group 16[85] ligands. Table III contrasts the d^0 and d^6 halides in this respect. Quite strong deshielding of the metal nucleus is observed in all the d^0 tetraoxo species from VO_4^{3-} to RuO_4,[46] and the shielding decreases in the sequence O > S > Se > Te whenever these species are measured.[37,44] The difference from main-group shielding is dramatic: thus, carbon shielding is highest in CI_4, whereas titanium shielding in lowest in TiI_4.

Dominance of the ΔE term must be favored in tetrahedral complexes as the ligand field splitting is $^4/_9$ that for analogous octahedral coordination, and the nephelauxetic effect of four ligands less than for six. Small differences in a small ΔE may then bulk large, giving large shifts.

The nephelauxetic sequence Cl < Br < I has been called "normal halogen dependence", and the opposite, spectrochemical, sequence "inverse halogen dependence",[12] although both extend to ligating atoms from neighboring groups. The behavior of fluorine, as a second-row element, is often anomalous.

B. The Nephelauxetic Series

The nephelauxetic parameter β, like Δ, is derived from optical spectra.[31] The wavenumber of the first (lowest energy) spin-allowed d–d band gives the splitting Δ, and the interval between the first and second band is a function of the interelectron repulsion, systematized by the Racah parameters. β is usually defined as the ratio of the values of the Racah B parameter in the complex and in the gaseous metal ion. The nephelauxetic sequence of increase in $(1 - \beta)$ and in the d-electron radius is given as F^- < H_2O < urea < NH_3 < en $\simeq$ ox^{2-} < NCS^- < CN^- $\simeq$ Cl^- < Br^- < I^- < dtc^- < dtp^- < $dsep^-$ < diars.[31] (The last four ligands are diethyl dithiocarbamate, dithiophosphate and diselenophosphate, and 1,2-(dimethylarsino)benzene.) Thus, for a given metal ion the nephelauxetic effect tends to decrease across the row of the table (as C > N > O > F, etc.) but to *increase* down the group (as F < Cl < Br < I, O < S < Se < Te, N < P < As < Sb), although the expression as a series of ligating atoms is less reliable than for the spectrochemical series. Certain ligands are more sensitive than others to the nature of the metal ion; thus, the interaction of a strong π-acceptor such as cyanide increases with increase in the number of d electrons and decreases with increase in effective nuclear charge on the metal.

For a given metal ion the nephelauxetic effect increases with decrease in electronegativity of the ligand, with increase in ligand reducing power and polarizability, and with increase in covalency of the M–L bond (as, for example, acceptance of σ, π charge from the ligand into the metal s, p, d orbitals expands the d electron cloud).

We have, therefore, an interesting difference in periodicity. *The spectrochemical and nephelauxetic effects reinforce for ligating atoms from the same row*, this explaining the linearity of δ/λ correlations for second-row ligands and the difficulty of extrapolation to a meaningful origin. *Down the group of the ligating atom, however, spectrochemical and nephelauxetic effects are usually opposed* (with an exception from nitrogen to phosphorus). This explains the decreasing slope of the δ/λ plot for ligands from successive rows, and other anomalies.

C. Quantification of Spectrochemical and Nephelauxetic Effects

The nephelauxetic ratio β has been incorporated in the shielding equation for a series of cobalt(III) complexes.[35] The radial function was expressed as $\langle r^{-3} \rangle_d/\beta$ and the energy term as h/β, where h is the energy of the first d–d band. The parameters were obtained from optical spectroscopic data by intermediate field calculations, giving an internal field strength (h/β) series of cobalt shielding, F^- < H_2O < Cl^- < $\simeq$ Br^- < NH_3 < CN^-, in which the heavier halides are moved forward by their nephelauxetism from their spectrochemical positions. Orthoaxial complexes (in which the ligands lie on the Cartesian axes) gave a good linear relation

TABLE IV. Periodicity of the Spectrochemical Parameter f and the Nephelauxetic Parameter h (eq 4 and 5) for Representative Ligands[a]

	C		N		O		F	
f	CN^-	≈1.7	NH_3	1.25	H_2O	1.0	F^-	0.9
	CO	≈1.8	en	1.28	ox^{2-}	0.99		
	π-C_2H_4	≈1.4	py	1.23	urea	0.91		
h	CN^-	2.0	NH_3	1.4	H_2O	1.0	F^-	0.8
			en	1.5	ox^{2-}	1.5		
					urea	1.2		
			P		S		Cl	
f			PR_3[b]	≈1.25	dtp^-	0.83	Cl^-	0.78
			$P(OR)_3$	≈2				
h					dtp^-	2.7	Cl^-	2.0
			As		Se		Br	
f			diars	1.33	$dsep^-$	0.8	Br^-	0.72
h						3.0		2.3

$h(I^-) \approx 2.7$

[a] f and h are dimensionless and scaled to unity for the hexaaquo ion. The value of the parameter is a property of 6L, or 3(LL) for bidentate ligands, as determined from d-d bands in $[ML_6]^q$ complexes. (The values for bidentate ligands may include effects of bond angle distortion, etc.) [b] R = Et, Ph.

between the cobalt magnetogyric ratio and h/β, extrapolation of which gave a good value of γ for the cobalt nucleus. The results with nonorthoaxial complexes such as $[Co(en)_3]^{3+}$ were, however, less regular.[35] Significant shifts are often observed for distorted geometries, as with chelating or bulky ligands.

A further example of the difficulties that arise in attempts to quantify these important relationships is the question of the power to which β should be raised. The linear relation established the constancy of $\langle r^{-3}\rangle_d/\beta$ for the orthoaxial complexes. But Coulomb repulsion follows an (r^{-1}) law; should not the appropriate power be the cube? Interestingly, rhodium salts in Rh(III) complexes with H_2O, Cl, Br ligands are better described by an optical parameter containing β^3 rather than β.[35]

The ab initio calculations of d-orbital contributions to the ^{55}Mn shielding in $[Mn(CO)_5L]$ complexes show that the shielding increases with decrease in $\pi(L \rightarrow M)$ donation, as Cl > CH_3 > H > CN (corresponding to increase in ligand field splitting). The shielding increases also as L becomes a harder ligand, $H^- \simeq CN^- < CH_3^- < Cl^-$, reducing the interaction with the soft Lewis acid $[Mn(CO)_5]^+$.[32]

A useful quantification of spectrochemical and nephelauxetic effects has been achieved by Jørgensen by the analysis of optical spectra of complexes with open d shells.[31] Remarkably, the octahedral splitting Δ_o can be written as a product of two functions (eq 4) and the

$$\Delta_o = f(\text{ligands}) \times g(\text{central ion}) \quad (4)$$

$$(1 - \beta) = h(\text{ligands}) \times k(\text{central ion}) \quad (5)$$

nephelauxetic effect similarly (eq 5) such that the f and h values order the ligands in the spectrochemical and nephelauxetic, series respectively, and the g and k values order the metal ions similarly. Tables IV and V show the periodicities of these parameters. In Table IV the f and h parameters both decrease from left to right across the row of the ligating atom, with reinforcing (deshielding) effects. the spectrochemical parameter f also decreases, gently, down groups 17 and 16, whereas the nephelauxetic parameter g increases markedly, by a factor of 3 or more.

These results illustrate the transferability of spectrochemical and nephelauxetic parameters between chromophores. The calculation of ligand field splittings in terms of parameterized contributions from M–L σ, π, δ, etc., bonding is systematized in the angular overlap model.[31]

D. Periodicities in Chemical Shift Additivities

Regular increments in the metal nucleus shift are often observed with successive substitutions of similar ligands, as in polyhalide complexes, mixed oxothio anions, M(0) complexes with mixed phosphine, carbonyl, etc., ligands, and so on. Such relationships have practical value in the identification of species in solution. There are regularities also in the size of increment: thus, the Br–Cl increment in Pt(IV) hexahalides is about half the I–Br increment, in a nephelauxetic sequence. Similarly the S–Se increment in BC_4^{3-} ions (B = V, Nb, Ta; C = S, Se, Te) is half the Se–Te increment, in a spectrochemical sequence.[37] Parallels can thus be drawn with the periodicities of the optical parameters.

A related additivity is that of ligand contributions to the electric field gradient at the metal center, as probed by nuclear electric quadrupole effects in NMR, NQR, or Mössbauer spectroscopy.[16] Departures from addi-

TABLE V. Periodicity of the Parameters g and k Expressing the Ligand Field Splitting ($\Delta = fg$) and Nephelauxetic Effect [$(1 - \beta) = hk$] of the Metal (eq 4 and 5)[a]

	V(II) d^3	Cr(III) d^3	Mn(IV) d^3	Mn(II) d^5	Fe(III) d^5	Co(III) d^6	Co(II) d^7	Ni(IV) d^6	Ni(II) d^8	Cu(III) d^8
g	12.0	17.4	24	8.0	14.0	18.2	9	22	8.7	15.7
k	0.08	0.21	0.5	0.07	0.24	0.35	0.13		0.12	
		Mo(III) d^3	Tc(IV) d^3	Ru(II) d^6		Rh(III) d^6		Pd(IV) d^6		Ag(III) d^8
g		24.6	31	20		27.0		29		20.4
k		0.15				0.3				
			Re(IV) d^3		Os(III) d^5	Ir(III) d^6		Pt(IV) d^6		
g			35			32		36		
k			0.2		≈0.28	0.3		0.5		

[a] g is in units of 1000 cm^{-1}; k is dimensionless.

tivity may be indicative of ligand interactions. Additivities of substituent shifts, and departure from this, are well-known for main-group compounds also.

E. Periodicities in Spectrochemical and Nephelauxetic Effects of the Metal

Table V shows the periodicities of the Jørgensen parameters g and k, which express relative tendencies of the metal ions to split the ligand field and to expand the d shell, following eq 4 and 5. Compared with the ligand parameters, the metal ion parameters show a greater range of variation, since each increases significantly with increase in oxidation number of the metal. This is of particular interest to the NMR spectroscopist, in view of the importance of the oxidation state in determining the likelihood of nephelauxetic, spectrochemical, or mixed ordering of the shifts.

Table V shows that the metal contribution (g) to the ligand field splitting increases from left to right across the table, for a given d configuration, with decrease in atomic radius. Down the group the ligand field splitting increases markedly, by about 50% from the first series to the second and 75% from the first to the third, with increase in covalent bonding. Since the effect of increase in Δ is to reduce the paramagnetic circulation and δ, this "spectrochemical" periodicity of the metal acts in opposition to that of the radial term. Also in opposition, as they affect the shielding, is the increase in g and in $\langle r^{-3} \rangle_d$ with increase in oxidation number.

The metal contribution (k) to the nephelauxetic effect, also, increases from left to right across the table (for a given d configuration), as the d orbitals contract and interelectron repulsion increases. But again, the periodicities differ in the trend down the group: the metal nephelauxetism changes rather little, decreasing slightly, as the d orbitals become more diffuse. This property, also, tends to oppose the effect on the metal shielding of the increase in the (atomic) radial term down the group.

Such differences from the main-group elements can explain the inconsistencies in the group trends in the transition series, as shown in Figure 1. The most important factor reducing shift ranges or sensitivities in the second and third series compared to the first appears to be the greater ligand field splittings after the first series.

Table V shows that a strongly nephelauxetic shielding pattern is to be expected at the end of the transition series, say with Pt(IV), for which the g and k values are both large. Indeed, the whole range of platinum shielding is spanned by the $[PtX_6]^{2-}$ halides, the shielding increasing from fluoride to iodide. It is a general observation that the shielding of transition metals (particularly later in the series) in lower oxidation states shows nephelauxetic ligand dependence, whereas transition metals in high oxidation states, earlier in the series, show spectrochemical ligand dependence, as further discussed below. Both sequences can be shown by the same metal: thus, ^{95}Mo and ^{183}W shifts show nephelauxetic ordering (as Cl < Br < I) in d^6 compounds, e.g. with phosphine or carbonyl coligands, and spectrochemical ordering O > S > Se in the metalates as so far measured,[44,47] and similarly for vanadium.[8]

F. Early and Late Transition Elements

Spectrochemical ligand dependence is relatively uncommon and can always be linked with low-energy magnetically active excitations. These may be mediated by low-lying d orbitals early in the transition series or by valence p orbitals at the end of the series. Spectrochemical ordering is found for certain d^{10} species, such as Ag(I) in the solid halides,[48] and Cu(I) (although other d^{10} compounds of the later transition elements, including Cd and Hg, show nephelauxetic ordering).[1-14] A small number of examples can be found in main-group chemistry, as in the alkali metals, which have low-lying p orbitals. It is found in certain compounds with low-lying $n \rightarrow \pi^*$ states, as in acid halides RCOX in oxygen resonance[49] (though not in carbon resonance, since the lone pair is on the oxygen), in nitrogen resonance in nitrosyl halides NOX or diazenes XN=NX,[43] and in cyclophosphazenes $(N{=}PX_2)_n$, though not in phosphorus resonance.

Inverse halogen dependence has been linked[12] with sign change in spin–orbit coupling (inversion of the multiplet) at the half-filled subshell, on the grounds that the valence orbital set is less than half-full in the free atoms K (s^1), Sc (d^3), Ti (d^4), V (d^5), and Cu ($d^{10}s^1$).[12] The presence of low-lying magnetically active excitations (particularly in the tetrahedral compounds) can, however, account for the inverse ordering.

That the inverse dependence observed for the formally d^0 metalates is associated with low excitation energies is exemplified by the semiconductor properties of the A_3BC_4 compounds with C = S, Se, or Te, and A = Cu, or Tl, studied in resonance of the B nucleus, V, Nb, or Ta.[37] More generally, the metalates in which the metal nucleus is quite strongly deshielded are deeply colored, permanganate ion for example, which shows the temperature-independent paramagnetism explained by Van Vleck in terms of low-lying magnetically active electronic states.[50] In the O, S, Se-substituted compounds the low-energy electronic absorption moves to longer wavelengths as the metal shielding decreases, and this was noted also for the ^{17}O shielding.[51]

As demonstrated by the MO theory for permanganate,[52] the main contribution to the susceptibility is from ligand field (mainly $1t_2 \rightarrow 2e$) excitations of oxygen σ- and π-bonding electrons in low-lying d orbitals. These excitations therefore dominate the metal nucleus shielding. The oxygen shifts in transition-metal tetraoxo compounds from VO_4^{3-} to OsO_4 were interpreted in terms of corresponding ($t_1 \rightarrow 3t_2$) circulations of nonbonding electrons on oxygen.[51] Such excitations are not, in fact, responsible for the color, which is due to a low-energy nonmagnetic ($t_1 \rightarrow 2e$) excitation, but the three bands move to lower energies and the shielding to higher frequencies in concert.

In formally d^0 complexes, therefore, the metal nucleus shielding is mediated by d–d circulations made possible by L → M charge transfer. In d^{10} complexes, similarly, M → L charge transfer may leaves holes in the d shell which allow d–d excitation, and low-lying np orbitals also come into play. Orgel remarked[53] that d–s mixing is favorable in Cu(I), Ag(I), Hg(II), Tl(III), etc., and s–p mixing in Pb(II), formally $d^{10}s^2$, to account for the low coordination numbers observed, such mixing being detectable by marked paramagnetic contributions to the susceptibility and the NMR shift.

TABLE VI. Angular Momentum Operations on the d Orbitals[55]

$\hat{l}_x d_{xz} = -i d_{xy}$	$\hat{l}_y d_{xz} = i d_{x^2-y^2} - i(3^{1/2} d_{z^2})$	$\hat{l}_z d_{xz} = i d_{yz}$
$\hat{l}_x d_{yz} = i(3^{1/2} d_{z^2}) + i d_{x^2-y^2}$	$\hat{l}_y d_{yz} = i d_{xy}$	$\hat{l}_z d_{yz} = -i d_{xz}$
$\hat{l}_x d_{xy} = i d_{xz}$	$\hat{l}_y d_{xy} = -i d_{yz}$	$\hat{l}_z d_{xy} = -2i d_{x^2-y^2}$
$\hat{l}_x d_{x^2-y^2} = -i d_{yz}$	$\hat{l}_y d_{x^2-y^2} = -i d_{xz}$	$\hat{l}_z d_{x^2-y^2} = 2i d_{xy}$
$\hat{l}_x d_{z^2} = -i(3^{1/2} d_{yz})$	$\hat{l}_y d_{z^2} = i(3^{1/2} d_{xz})$	$\hat{l}_z d_{z^2} = 0$

The ab initio study[33] of metal nucleus shifts in complexes of Cu, Ag, Cd, and Zn concluded that the d mechanism is predominant for Cu, the shielding decreasing with increase in $\pi(M \rightarrow L)$ charge transfer as $Cl < NH_3 < CN$, whereas the p mechanism is dominant for Zn and Cd, the shielding decreasing with decrease in ligand electronegativity, as $H_2O > Cl > CH_3$. For Ag the d and p mechanisms are competitive. Again, we see a periodic dependence, since the trends depend on the energy levels of the free metal atoms, as they determine the energy intervals in question.

In Pt(0) complexes with alkyne and phosphine ligands, similarly, the role of d–p mixing was demonstrated by EHMO calculations, and the decrease in platinum shielding with decreasing energy of the $d(xz, x^2 - y^2) \rightarrow \delta^*$ excitation, the LUMO being formed from d and alkyne π^* orbitals.[54]

IX. Solid-State Studies

The elements of the shielding tensor measured in oriented molecules are given by[19]

$$\bar{\sigma} = (\sigma_{11} + \sigma_{22} + \sigma_{33})/3$$

where $\bar{\sigma}$ is the averaged value, as obtained in the liquid phase in the absence of solvation effects, and $\sigma_{11} < \sigma_{22} < \sigma_{33}$ by convention. There is a problem of sign convention, since the shielding σ, by the definition $B_{eff} = B_0(1 - \sigma)$, is more positive to lower frequency (higher field): the *shielded* nucleus experiences a *reduced* field B_{eff}. The shielding σ is thus opposite in sign to the chemical shift δ as now defined. Some recent work has used the high-frequency positive convention with the symbol σ (=s for shielding); but if this convention is preferred, the elements so given are those of the shift tensor δ, not the shielding tensor σ.

For axial symmetry, the shielding anisotropy $\Delta\sigma$ is given by

$$\Delta\sigma = \sigma_{\parallel} - \sigma_{\perp}$$

or, more generally, by

$$\Delta\sigma = \sigma_{33} - (\sigma_{11} + \sigma_{22})/2$$

although other definitions of $\Delta\sigma$, e.g. $(\sigma_{33} - \bar{\sigma})$, are in use. A shielding asymmetry parameter is defined also:

$$\eta = (\sigma_{22} - \sigma_{11})/(\sigma_{33} - \bar{\sigma})$$

Table VI gives the angular momentum operations $\hat{l}$ on the d orbitals.[55] Thus, in a d^8 square-planar complex, with only the $d_{x^2-y^2}$ orbital unfilled, the shielding element σ_{zz}, corresponding to a magnetic field direction parallel to the fourfold (z) axis, generates $d_{xy} \rightarrow d_{x^2-y^2}$ circulations with excitation energy $\Delta E(^1A_1 \rightarrow {}^1A_2)$. Similarly a magnetic field parallel to the in-plane x (or y) axis generates $d_{yz} \rightarrow d_{x^2-y^2}$ (or $d_{xz} \rightarrow d_{x^2-y^2}$) circulations with excitation energy $\Delta E(^1A_1 \rightarrow {}^1E)$, giving rise to the σ_{xx} (or σ_{yy}) element. The shielding tensor is then axially symmetric; but with mixed ligands in the plane the degeneracy of the d_{xz}, d_{yz} orbitals and of the ^1E state is lifted and the tensor becomes fully anisotropic.

Thus, each shielding element is mediated by a ligand field ($d\pi \rightarrow d\sigma^*$) circulation *in the plane perpendicular to the axis of that element*. As we have seen, d–d contributions are usually important in formally d^0 complexes and may be so in d^{10} complexes; and p–p contributions become important for late-transition elements.

For anisotropic site symmetries, therefore, knowledge of the tensor components allows a much more precise description of the chemical shift. Solid-state techniques are important also for insoluble materials (ceramics, catalysts, etc.) and for bio-NMR work.

High-resolution NMR spectroscopy of solids has flowered in recent years, with a combination of techniques for line-narrowing and sensitivity enhancement for less receptive nuclei.[18,19] Direct dipolar interactions and shielding anisotropies that do not average to zero in oriented samples are greatly reduced by magic angle spinning MAS (or some special pulse sequences), and high-power rf decoupling can be used both for reducing dipolar interactions and for sensitivity enhancement by cross-polarization from protons (CP). Shielding tensors can, however, be recovered, by use of MAS at lower frequencies than the shielding anisotropy in hertz. The broad-line spectrum breaks up into a series of spinning side bands, and an analysis of the pattern of their intensities gives the shielding tensor elements.[56] The contribution of such techniques to the study of ligand effects in the shielding of transition-metal nuclei has been limited as yet by the technical problems, but the field is now ripe for development (with expertise!). Anisotropies of the shielding tensor are reviewed annually.[31]

Some of the problems of the transition-metal nuclei, as illustrated in Table I, were discussed in section II. Of the 10 nuclei with spin $^1/_2$ several have rather low sensitivity, the most favorable ones being ^{195}Pt, ^{113}Cd, and ^{199}Hg; indeed, ^{195}Pt has 20 times the receptivity of ^{13}C. In general, for such work, the compounds for study must be carefully chosen to reduce line broadening and maximize sensitivity, e.g. by using cross-polarization techniques with organic ligands.

Of the 32 nuclei in Table I two-thirds have spin $I > {}^1/_2$, and the nuclear electric quadrupole poses greater problems in the solid than in the liquid phase.[18,19] They tend to be greater for heavier nuclei, with larger quadrupole moments (eQ) and electric field gradients (eq) at the nucleus. Except in highly symmetric environments (q small) the quadrupolar coupling to the efg (which averages to zero in the liquid phase) normally dominates the solid-state spectrum, multiplying, broadening, and shifting the lines.

Most favorable are nuclei with nonintegral spins, such as ^{27}Al with $I = {}^5/_2$, since the $({}^1/_2, -{}^1/_2)$ spin transition is independent of the alignment of the efg tensor relative to the magnetic field and so is free of quadrupole effects to first order. The second-order effects remain, shifting and broadening the lines, and are reduced but not eliminated by MAS. Variable-angle or off-(magic-angle) sample spinning (VASS)[57] is sometimes useful but does not minimize other sources of line broadening (dipolar interactions, shift anisotropy), and complex patterns may be obtained. Higher fields are advanta-

TABLE VII. Shielding Tensors (ppt, ±0.2) for Transition-Metal Nuclei with Spin $I > 1/2$

	$\bar{\sigma}$	σ_{xx}	σ_{yy}	σ_{zz}	$\Delta\sigma$	NQCC, MHz	η	λ_{max}, Å	ref
				^{59}Co (ref $K_3[Co(CN)_6]$					
$[Co(CO)_4Mn(CO)_5]$, d^8	3.0	3.0	3.0	3.1	0.1	128.7[a]	0.12[a]		61
$[Co(CO)_4SnPh_3]$, d^8	3.2	3.3	3.2	3.1	−0.1			2700	59
$[Co(CO)_4SnBr_3]$, d^8	2.6	2.4	2.3	3.0	0.65			3038, 2675	59
$[Co(CO)_4GeI_3]$, d^8	2.3	1.9	1.8	3.1	1.3			3919, 3119	59
$[Co(CO)_3(\mu\text{-}CO)]_2$, d^8	2.2	2.4	2.4	1.9	−0.5	89.7[a]	0.40[a]		64
$[CoCp_2]NO_3{\cdot}H_2O$, d^6	2.5	0.2	0.5	6.7	6.35	165.6	0.007		58
trans-$[Coen_2(NO_2)_2]NO_3$, d^6	−6.3	−6.2	−6.5	−6.1	0.25	13.2	0.727		58
$[Co(NH_3)_5CN]Cl_2$, d^6	−6.7	−6.0	−5.9	−8.2	−2.25	26.6	0.185		58
trans-$[Coen_2Cl_2]Cl{\cdot}HCl{\cdot}2H_2O$, d^6	−9.2	−10.6	−10.9	−6.1	4.65	71.7	0.225		58
$[Co(NH_3)_4CO_3]Br$, d^6	−9.7	−9.9	−10.4	−8.9	1.25	18.8	0.727		58
				^{55}Mn (ref MnO_4^-)					
$[Mn(CO)_5Re(CO)_5]$, d^8	2.55			small		8.67	0.61	3112	62
$[Mn(CO)_5GePh_3]$, d^8	2.4	2.3	2.3	2.5	0.2				63
$[Mn(CO)_5]_2$, d^8	2.3	2.3	2.4	2.3	0.0	3.28	0.36	3410	62
$[Mn(CO)_5Co(CO)_4]$, d^8	1.6	1.5	1.5	1.9	0.4	−19.9	0.004	3490	61, 62
$[MnCp(CO)_5]$, d^6	2.3	2.0	2.0	3.0	1.0	64.3	0.01		60
$[Mn(CO)_6]^+$, d^6	1.51				0.0				60
$[Mn(CO)_5I]$, d^6	1.3	1.0	1.0	2.0	1.0	19.8	0.02		60
$[Mn(CO)_5Br]$, d^6	1.1	0.6	0.7	1.9	1.2	17.5	0.04		60
$[Mn(CO)_5Cl]$, d^6	1.0	0.5	0.6	1.9	1.3	13.9	0.04		60
				^{187}Re (ref ReO_4^-)					
$[Re(CO)_5]_2$, d^8	4.2	4.4	4.2	3.9	0.3	134.0	0.63		62

[a] Averaged values for nonequivalent lattice sites.

geous, giving a reduction in quadrupolar effects (which are inversely proportional to the field strength) as well as better shift dispersion. But in contrast to the interest focussed on ^{27}Al in aluminosilicates (which cannot be studied in solution), there has been rather little MAS study as yet of quadrupolar transition-metal nuclei, although preliminary results were reported for ^{51}V in V_2O_5 (with $\Delta\sigma \simeq 1000$ ppm) and ^{93}Nb in $NaNbO_3$, with relatively small efg.[57]

Most desirable is NMR study of oriented single crystals in which the molecular structure is known from X-ray crystallography. For quadrupolar nuclei, useful comparison can be made also with the efg tensor (determined by NQR), since the shielding and efg tensors have the same dependence on the ground-state charge distribution, in the approximate descriptions of eq 1–3. Inear σ/NQCC relationships are then possible if the effective excitation energies are similar (or vary in parallel).[15,16] Important but neglected single-crystal work that was done by Spiess, Sheline, and others[58–64] before the general availability of modern CP-MAS techniques is shown in Table VII. They measured a range of ligands in d^6 and d^8 complexes of ^{59}Co, ^{55}Mn, etc. The compounds are arranged in general order of decreasing overall shielding ($\bar{\sigma}$), although certain groups are listed together for comparison. The component along the axis of highest symmetry is labeled σ_{zz}, following the convention for the efg. The asymmetry of the efg (η), which takes a maximum value of 1 and is 0 for axial symmetry, may show nonzero values in compounds that are in fact axially symmetric, because of lattice distortions; and doublings may arise from the presence of two lattice sites, averaged values being given in Table VII. The shifts are large and expressed in parts per thousand (ppt).

For cobalt the highest shielding (6.7 ppt), observed for the axial direction of the d^6 cobalticenium ion $[CoCp_2]^+$, is related to the high (near-cylindrical) symmetry and lack of low-lying excited states, and this ion shows the highest anisotropy (6.35 ppt).[58] Higher overall shieldings are observed in the d^8 carbonyls,[59,61] related to high excitation energies for the strong CO ligand, and for the d^8 configuration. In the series of $(CO)_4Co$–M binuclear compounds the σ_{zz} value (with the z axis parallel to the Co–Mo bond) is effectively constant at 3.1 ppt; and the perpendicular values increase as $GeI_3 < SnBr_3 < SnPh_3$, with decrease in λ(d–d).[59,61] In $[Co_2(CO)_8]$,[64] however, the σ_{zz} element shows relatively low shielding, with two bridging carbonyl ("inorganic ketone") groups. This result has added interest because solutions of this compound contain other (e.g., nonbridged) structures in equilibrium.

Among the d^6 octahedral complexes[58] the anisotropy $\Delta\sigma$ varies in linear fashion with the NQCC. The largest deshielding is observed for the tensor components sensitive to the weak ligand Cl in *trans*-$[Co(en)_2Cl_2]$, which shows the largest anisotropy. Highest shielding is observed for the strongest ligand CN. The σ_{zz} values show significantly higher shielding for two ethylenediamine ligands in the plane (−6.1 ppt) than for four NH_3 ligands (−8.2, −8.9 ppm), and this is attributable in good measure to chelate effects. The different values for the two tetraammines illustrate a general observation, of indirect influences of ligands that do not contribute directly to a particular tensor element. Such influences include (σ, π) inductive effects transmitted by the metal, and steric effects of angle distortion.

Corresponding results were observed in ^{55}Mn resonance.[60–63] Highest shielding is observed for σ_{zz} in $[MnCp(CO)_5]$,[60] with high symmetry and strong ligands. In the $Mn(CO)_5$–M series, with metal–metal bonds and no bridging carbonyls, all the tensor elements increase as Co < Mn ≃ Ge (<Re, probably), with decrease in wavelength of the longest wavelength UV band, attributed to $\sigma \rightarrow \sigma^*$ excitation in the metal–metal bond.[61–63] In the d^6 compounds[60] the anisotropy increases as the shielding decreases, as CO > I > Br > Cl. The d–d bands, at relatively high energy, are masked by charge-transfer bands, but the shielding sequence was related to PES evidence of diminishing 3d partic-

TABLE VIII. Shielding Tensors (ppm) for Transition-Metal Nuclei with Spin $^1/_2$

	$\bar{\sigma}$	σ_{11}	σ_{22}	σ_{33}	$\Delta\sigma$	coord sphere	ref
			^{113}Cd, d^{10} (ref $Cd(ClO_4)_2$)				
$[Cd((Me_2N)_2CS)_2(NO_3)_2]$	−98	−327	−307	340	657	O_4S_2[a]	67
$[Cd(glycinate)_2]\cdot H_2O$	−113	−256	−200	116	344	O_3N_2[a]	67
$[Cd(S_2COEt)_2]$	−410	−583	−386	−262	222	tetrahedral[a]	69
[Cd(TPP)][b]	−399	−626	−285	−285	−341	planar	68
[Cd(py)(TPP)]	−432	−502	−397	−397	−105	N_5	68
			^{183}W (ref WO_4^{2-})				
$H_3[W_{12}O_{40}P]$, d^0	174	−409	−148	1079	1357	oct	71
			^{195}Pt (ref $K_2[PtCl_6]$)				
cis-$[PtCl_4(NH_3)_2]$, d^6	237	134	209	367	170	oct	66
cis-$[PtMe_2(PEt_3)]_2$, d^8	4654	4261	4644	5056	603	planar	66
columnar, d^8	$\bar{\sigma}$	$\sigma_\parallel$		$\sigma_\perp$	$\Delta\sigma$	coord sphere	ref
$K_2[Pt(CN)_4]\cdot 3H_2O$	4870	3400		5600	−2200	planar	65b
$Ba[Pt(CN)_4]\cdot 4H_2O$	5100	3400		5930	−2500	planar	65a
$[Pt(NH_3)_4]Cl_2\cdot H_2O$	2070	−3000		4600	−7600	planar	65a
$K_2[Pt(C_2O_4)_2]\cdot 2H_2O$	1130	−4600		4000	−8600	planar	65a
$K_2[PtCl_4]$	1799	−5143		5270	−10414	planar	65a
	1400	−5600		4900	−10500	planar	65c
$K_2[Pt(CN)_4]Br_{0.3}\cdot 2.3H_2O$	870	0		2600	−2600	planar	65b

[a] Distorted. [b] *meso*-Tetraphenylporphin.

ipation in the dπ HOMO down the group of the halogens, decreasing the contribution to σ_{xx}.[60,62]

The σ_{zz} component is constant within the series (at 1.9–2.0 ppt), being independent of the substituent, but differs significantly from the values observed for $[Mn(CO)_6]^+$ (1.5) and the $Mn(CO)_5$ dimer (2.3). The lower shielding in the cation and higher axial shielding in the Mn–Mn compounds are consistent with the conclusions from MO calculations on the d^6 hexacarbonyls of V, Cr, and Mn that M–CO back-bonding decreases across the row with increase in oxidation number of the metal, decreasing ΔE and increasing the 3d participation in the HOMO, and so reducing the shielding.[60,62]

Table VIII gives anisotropic shielding tensors observed for spin $^1/_2$ transition-metal nuclei, including single-crystal work on compounds of platinum[65a–c] and cadmium.[67,68] Powder patterns can often be interpreted unambiguously, with the wealth of information from solution studies.[66–71] Most attention has so far been paid to platinum[65a–c] and cadmium[67–70] because of the favorable NMR properties and the chemical properties of cadmium related to those of zinc and calcium, which are much more difficult to study by NMR (^{43}Ca has a natural abundance of 0.145%). Solutions raise problems of fast ligand and solvent exchange, and the possibility of protein-binding studies has promoted interest in ligand environments that may resemble those found in enzymes.

Large shielding anisotropies have been observed for platinum in planar (d^8) complexes from solution studies of shielding anisotropy relaxation rates,[3] which increase as $(\Delta\sigma)^2B_0^2$. The anisotropy has been determined directly as −10.4 ppt in single crystals of K_2PtCl_4,[65a,c] with particularly low shielding for the out-of-plane component ($\sigma_\parallel$) which is sensitive to the four (weak) ligands.

Ligand field effects are shown very nicely by the series of square-planar complexes of Pt(II) in Table VIII. $\sigma_\parallel$ increases by 9 ppt with increase in the ligand field strength in the sequence $Cl^- <$ oxalate$^{2-} < NH_3 \ll CN^-$, and the anisotropy diminishes by 8 ppt across this range, since $\sigma_\perp$ varies much less.[65a] Still higher axial shielding and a smaller (absolute) magnitude of the anisotropy were measured more recently for the strong ligands Me and PEt_3.[66] Interestingly, the tetrachloro, -ammine, and -cyano complexes crystallize with infinite stacking of the planes (usually 45° staggered) to form columns parallel to the z ($\sigma_\parallel$) direction.

There is some increase in $\sigma_\perp$ (by 900–1200 ppm) from the ammine or the chloro complex to the cyanide, which no doubt involves ligand field effects. The increase in $\sigma_\perp$ was thought to be related to the decrease in the Pt–Pt distance (by 90 pm from the ammine to the cyano complex) and increase in unidimensional metallic character;[65a] but there is little correlation of the platinum shift with Pt–Pt distance in a series of tetracyano complexes of Pt(II), even when the metal ions approach so closely that the crystals become colored and the optical properties unidimensional, absorption and reflection bands being polarized in the direction of the metal chain.[65b]

Really close Pt–Pt approach, within 11 pm of that in platinum metal, can be achieved by partial oxidation, and the crystals then have a bronze luster and some electric conductivity.[65d] One such Krogmann salt in which the platinum has oxidation number +2.3 (with 0.3 Br^-) was measured as a large single crystal (cf. Table VIII). In comparison with the colorless $K_2[Pt(CN)_4]\cdot 3H_2O$, the platinum NMR changes in parallel with the optical properties. The Pt signals are broadened fourfold, and both the parallel and perpendicular tensor components shift by 3 ppt to higher frequencies. Such shifts are greater than normal Pt(II)–Pt(IV) chemical shifts, and resemble Knight shifts produced by conduction electrons, just as the broadening can be explained by electron–nuclear relaxation. Thus, the changes in nuclear magnetic shielding and relaxation, as in the optical properties, are related to electron delocalization by overlap of the incompletely occupied d_{z^2} orbitals along the platinum chain, these changes being reversible between the colorless and bronze forms. That the electron delocalization is confined to a region along the metal chain is shown by the proton resonance of the water in the crystal lattice, which does not differ significantly from that observed for corresponding colorless complexes of Pt(II).[65b] Thus, NMR can add to the information given by other physical techniques.

Of interest is 3-dimensional information of changing ligation, including effects of chelation. Thus, in Cd(TPP), as shown in Table VIII, the anisotropy at cadmium is −341 ppm. Addition of pyridine at one axial position reduces σ by only 33 ppm but reduces $|\Delta\sigma|$ by 136 ppm; interestingly, the axial shielding element (sensitive to ligands in the porphin plane) increases by 124 ppm, because the pyridine pulls the cadmium out of the plane.[68] Quite large anisotropies are reported for linear (2-coordinate) compounds of cadmium from liquid crystal or relaxation studies, larger still for analogous mercury compounds (by a factor of 2 or more, given the greater shift range for the heavier element); e.g. ca. 7000 ppm for $HgPh_2$.[3]

Many of the solid-state results confirm those that are familiar from solution work (while affirming potential value, e.g., for membrane studies). Thus, cadmium shielding increases with ionicity (longer bonds) or with coordination number for a given ligand (as well-known for other nuclei, such as tin). There are, of course, complications intrinsic to solid-state work, such as multiple resonances arising from nonequivalent lattice sites, and anisotropies or asymmetries observed for compounds for which octahedral site symmetry might be expected from the formula of the complex, because of distortions arising from the crystal packing, hydrogen bonding, chelation, varaiable puckering in chelate rings, etc.

The shielding patterns show that ligand field effects are relatively small for these late-transition elements. For cadmium, the metal shielding in solids[3,67-70] increases approximately as N < O for 6-coordination, and S < Se < Cl < Br < Te < I for 4-coordination (with varying chelation effects for bidentate sulfur ligands), the shifts for alkyl or aryl ligands occurring in the S, Se region. Again, the conclusions of the theoretical study apply,[33] that the deshielding depends largely on p–p circulations, increasing with electron donation from the ligand (the d–d contributions becoming significant with back-bonding ligands).

The potential for work with lower γ nuclei, despite long relaxation times, has been demonstrated in the case of ^{183}W.[71] Table VIII shows the shielding tensor in the Keggin polytungstate $H_3[P(W_{12}O_{40}].nH_2O$, which has 12 equivalent tungstens, each octahedrally coordinated by oxygen, with phosphorus at the center. Interestingly, low shielding is observed for the equal tensor elements sensitive to the electronegative substituent. This agrees (according to the theory of the shielding in d^0 metalates discussed in section VIIIF) with the evidence of UV and redox potential studies[72] that the first charge-transfer band moves to longer wavelength (and the oxidative capacity increases) with a more electronegative heteroatom (P vs. Si) inside the Keggin polyanion.

X. Dependence of the Shielding on Metal Oxidation State and M–M Bond Order

Deshielding with increase in oxidation number, as with decrease in electron density, is commonly observed for main-group and transition elements and correlates with increase in the radial function. Optical spectroscopy shows an increase in the metal g and k parameters with increase in oxidation number, indicating that ligand effects are of greater importance. In transition-metal nucleus shielding, the low-frequency (high-field) range is occupied by M(0) complexes of strong neutral ligands (CO, phosphines, PF_3, etc.); but very high metal shielding is observed also for complexes with small η^n- rings. Examples are the piano stool compound $[FeCb(CO)_3]$ (Cb = cyclobutadiene),[73] $[MCp_2]^q$ sandwiches (M = Fe,[74] Co, Ru,[46] Rh), and bent sandwich compounds $[MCp_2H_2]$ (M = Mo, W, etc.), and these have formal oxidation numbers up to +4. Furthermore protonation, e.g. to $[FeCp_2H]^+$ or $[MoCp_2H_3]^+$, significantly increases the metal nucleus shielding and also the formal oxidation number, up to +6. Thus, complexes with highest shielding may have high oxidation numbers and a d^0 or d^2 configuration, and may be positively charged.

These "anomalies" can be related to the MO diagrams. In sandwich and piano stool compounds the metal shielding increases with increase in the ligand field splitting as the ring becomes smaller and more strongly bound, through better matching of the M(d) and ring 2pπ orbital energies, for which there is PES evidence.[75] Protonation increases the metal shielding by stabilizing (nearly) nonbonding d electrons in M–H σ bonds;[47] an analogue is the protonation of nitrogen in delocalized systems (as in pyridine), which increases the nitrogen shielding by stabilizing the nitrogen lone pair electrons.[43] An interesting question is that of the nephelauxetic effects of η^n ligands, to be discussed in the general context of coordination shifts.[76]

Effects of change in local symmetry, also, are to be expected. For quadrupolar metal nuclei this can be monitored by changes in the NQCC, as already discussed, through its dependence on the efg at the nucleus, which decreases with increase in local electronic symmetry. The NQCC (χ) can be estimated from the NMR line width or quadrupolar relaxation rate (both proportional to χ^2). Cyclopentadienyl complexes commonly give sharp lines,[77] and broader lines are observed for mixed sandwich compounds.[75]

At low shieldings, also, there are "anomalies" readily explained in MO terms. Thus, the lowest shielding observed for molybdenum or tungsten so far (lower than in the d^0 metalates) is in the formally M(II) dimers with quadruple M$\equiv$M bonds.[44] The low shielding can be related to small excitation energies ($\sigma \leftrightarrow \pi$, $\pi \leftrightarrow \delta$, etc.) and considerable angular imbalance of charge, as evident in the quadrupolar broadening. As expected, the metal shielding is higher in $[Mo_2X_4(phos)_4]$ (X = Cl, Br, I) complexes than in the carboxylates $[Mo_2(O_2CR)_4]$,[47] in which it decreases with decrease in pK_a of the carboxylic acid;[44] but the ^{95}Mo shifts in $[Mo_2X_8]^{4-}$ (X = Cl, Br) and $[Mo_2X_4(phos)_4]$ (X = Cl, Br, I) show a quasi-nephelauxetic dependence, perhaps with some relativistic contribution, as discussed below.

Interestingly, in Mo–Mo-bonded compounds with comparable ligands the metal shielding decreases steadily with increase in bond order, as Mo—Mo > Mo=Mo > Mo≡Mo > Mo$\equiv$Mo,[47] in contrast to the well-known single > triple > double bond sequence found in carbon[25] or nitrogen[43] shielding. The ^{95}Mo quadrupolar broadening tends to increase with the multiplicity, and excitation energies are likely to decrease with the decrease in overlap from σ to π to δ orbitals, so the monotonic order is to be expected. It

is the second-row ordering that is anomalous, in fact an effect of local symmetry. It arises from the free diamagnetic circulation about the triple-bond axis,[25] which is not possible for transition metals with nonlinear coordination.

XI. Relativistic Effects in Transition-Metal Shielding

Effects of relativity must play a significant part in the shielding of the heaviest nuclei. An electron close to a heavy nucleus reaches velocities near that of light, so that its mass and binding energy increase and the radius decreases, depending on the its penetration, i.e. s > p > d > for a given n, and also $np^{1/2} > np^{3/2}$; the spin-uncoupling increases sharply with atomic number, as Z^4/n^3. Chemical effects are direct and indirect.[78] Relativity contributes 10–15% to the lanthanide contraction, and by the end of the third transition series the increase in nuclear screening by the s, p contraction is sufficient to expand the 5d shell, making this more available for covalent bonding. Such arguments account for "anomalous" chemical properties of Au, Hg, and Tl, higher valencies for W compared to Mo, and so on.[78] The theory as applied to NMR shifts is difficult and is under development.[79]

Heavy atom *ligands* produce a spin–orbit shielding (LS) contribution σ_{LS} transmitted by a mechanism as for J coupling (so the interacting atoms must be dissimilar).[80] Paramagnetic currents on the heavy ligand produce spin polarization in the bonds to the central atom, and the Fermi contact of the bonding s electrons with the resonant nucleus stabilizes one of its spin states, in proportion to applied field. This was proposed[81] and calculated for halogens bonded to protons[82] or carbon.[83,30] The σ_{LS} contribution to the carbon shielding is 307 ppm in CI_4, cf. 76 ppm in CBr_4 and 12 ppm in CCl_4.[83]

The heavy-neighbor spin–orbit contribution has not as yet been studied in transition-metal complexes (it has been suggested for ^{207}Pb in PbTe[84]). It is highly sensitive to low-lying excited states, as σ_{LS} is a third-order term, with an additional $(\Delta E)^{-1}$ factor for the singlet–triplet excitation. The effect must be sizable when there is polysubstitution by heavier ligands, but the ordering is the same as for the nephelauxetic effect, so the two can be confused. The next step will perhaps be elucidation of the spin contribution to the shielding of the heavy atom itself.

XII. Conclusions

Our analysis began with the three major factors in nuclear magnetic shielding, and the part played by the radial term in the periodicity of the shielding range of the elements. From the main-group to the transition elements, however, the ranges are amplified by the larger angular momentum factors $\langle 0|L^2|0\rangle$ for d than for p orbitals. The ranges for the first transition series (compared to the second and third) are further amplified by the smaller ligand field splittings. Thus, all three factors play a part.

Comparisons of transition-metal shifts usually assume rather little variation in the angular momentum factor, although sizable shifts may in fact be observed with departure from orthoaxial symmetry due to ring strain, bulky ligands, small ligands such as hydride, etc. In view of the ease with which the local electronic symmetry can be monitored for quadrupolar nuclei, by line width or other relaxation measurements, we may hope to see further studies of the less common geometries from this point of view.

The propensities of transition metals and ligands to split the ligand field and to expand the d shell in complexes play a key role in nuclear magnetic shielding as in electronic spectroscopy. The degree to which these propensities may be compared and estimated as transferable properties has been demonstrated for optical spectroscopy. The periodic relationships show that there is some transferability also between the two spectroscopies, and more semiquantitative studies are needed in this field as well.

The two spectroscopies are complementary in certain respects. The NMR spectroscopy in question is limited to diamagnetic compounds, but information from optical spectroscopy of high-spin and low-spin complexes is relevant to it. Reciprocally, ligand field effects in the NMR shifts of d^0 or d^{10} complexes, or others in which the d–d bands are unobservable, are relevant to optical spectroscopic theory. It would be helpful if more NMR spectroscopists would take in interest in the theory of electronic spectroscopy, and vice versa. The high dispersion of NMR shifts is valuable (and we have not discussed the further contributions from J coupling, relaxation, etc.) Each form of spectroscopy probes electronic structure and bonding in its own way: in due time the debt of NMR spectroscopy to optical spectroscopy and ligand field theory will no doubt be repaid.

XIII. References

(1) Mason, J., Ed. *Multinuclear NMR Spectroscopy*; Plenum: New York, 1987.
(2) Rehder, D. In Reference 1, Chapter 19.
(3) Goodfellow, R. J. In Refence 1, Chapters 20 and 21.
(4) Benn, R.; Rufinska, A. *Angew. Chem., Int. Ed. Engl.* **1986**, *25*, 861.
(5) Rehder, D. *Chimia* **1986**, *40*, 186.
(6) Von Philipsborn, W. *Pure Appl. Chem.* **1986**, *58*, 513.
(7) Dechter, J. J. *Prog. Inorg. Chem.* **1985**, *33*, 393.
(8) Rehder, D. *Magn. Reson. Rev.* **1984**, *9*, 125.
(9) Laszlo, P., Ed. *NMR of Newly Accessible Nuclei*; Academic: New York, 1983; Laszlo, P., Chapter 9; Mann, B. E., Chapter 11; Granger, P., Chapter 15.
(10) Kidd, R. G. In *The Multinuclear Approach to NMR Spectroscopy*; Chapter 21. Lambert, J. B., Riddell, F. G., Eds.; NATO ASI Series; Reidel: Dordrecht, 1983; Chapter 21.
(11) Davies, J. A. In *The Chemistry of the Metal-Carbon Bond*; Hartley, F. R., Patai, S., Eds.; Wiley: Chichester, 1982; Chapter 21.
(12) Kidd, R. G. *Annu. Rep. NMR Spectrosc.* **1980**, *10A*, 1.
(13) Rinaldi, P. L.; Levy, G. C.; Choppin, G. R. *Rev. Inorg. Chem.* **1980**, *2*, 53.
(14) Kidd, R. G.; Goodfellow, R. J. In *NMR and the Periodic Table*; Harris, R. K., Mann, B. E., Eds.; Academic: London, 1978; Chapter 8.
(15) Jameson, C. J.; Mason, J. In Reference 1, Chapter 3.
(16) Mason, J. *Adv. Inorg. Chem. Radiochem.* **1976**, *18*, 197; **1979**, *22*, 199.
(17) Ramsey, N. F. *Phys. Rev.* **1950**, *78*, 699; **1952**, *86*, 243.
(18) Harris, R. K. In *Nuclear Magnetic Resonance Spectroscopy; a Physicochemical View*; Pitman: London, 1983. Jameson, C. J.; Mason, J. In Reference 1, Chapter 2.
(19) Fyfe, C. A. In *Solid State NMR for Chemists*; C.F.C.: Guelph, Ontario, 1983; Mehring, M. *High Resolution NMR Spectroscopy in Solids*; Springer-Verlag: Berlin, 1976. Haeberlen, U. *Adv. Magn. Reson.* **1976**, Supplement 1.
(20) Le Bail, H.; Chachaty, C.; Rigny, P.; Bougon, R. *J. Phys. Lett.* **1983**, *44*, 1017.
(21) Jameson, C. J.; Gutowsky, H. S. *J. Chem. Phys.* **1964**, *40*, 1714.
(22) Barnes, R. G.; Smith, W. V. *Phys. Rev.* **1954**, *93*, 95.
(23) Moore, C. E. *Natl. Bur. Stand. Circ. (U.S.)* **1949–1958**, *1-3* (No. 467); revised 1971.
(24) Carlson, T. A.; Lu, C. C.; Tucker, T. C.; Nestor, C. W.; Malik, F. B. *Eigenvalues, Radial Expectation Values, and Potentials*

for Free Atoms from Z = 2 to 126 as calculated from Relativistic Hartree-Fock-Slater Atomic Wave Functions; Oak Ridge National Laboratory: Oak Ridge, TN, 1970.
(25) Karplus, M.; Pople, J. A. *J. Chem. Phys.* **1963**, *38*, 2803. Pople, J. A. *J. Chem. Phys.* **1962**, *37*, 53, 60; *Discuss. Faraday Soc.* **1962**, *34*, 7; *Mol. Phys.* **1963**, *7*, 301.
(26) Phillips, C. S. G.; Williams, R. J. P. *Inorganic Chemistry*; Oxford University: Oxford, 1965; Vol. 2.
(27) Mason, J. *J. Chem. Educ.*, in press.
(28) Griffith, J. S.; Orgel, L. E. *Trans. Faraday Soc.* **1957**, *53*, 601.
(29) Buckingham, A. D.; Stephens, P. J. *J. Chem. Soc.* **1964**, 2747, 4583.
(30) Schastnev, P. V.; Cheremisin, A. A. *J. Struct. Chem.* (*Engl. Transl.*) **1982**, *23*, 440.
(31) *Nucl. Magn. Reson.* **1972–1987**, *1–16*: Raynes, W. T., Vol. 1–8; Jameson, C. J., Vol. 9–16.
(32) Kanda, K.; Nakatsuji, H.; Yonezawa, T. *J. Am. Chem. Soc.* **1984**, *106*, 5888.
(33) Nakatsuji, H.; Kanda, D.; Endo, K.; Yonezawa, T. *J. Am. Chem. Soc.* **1984**, *106*, 4653.
(34) Stevens, K. W. H. *Proc. R. Soc. London, A* **1953**, *219*, 542.
(35) Griffith, J. S. *The Theory of Transition Metal Ions*; Cambridge University: Cambridge, 1961.
(36) Jørgensen, C. K. *Absorption Spectra and Chemical Bonding in Complexes*; Pergamon: Oxford, 1962; *Modern Aspects of Ligand Field Theory*; North-Holland: Amsterdam, 1971; *Prog. Inorg. Chem.* **1962**, *4*, 73 and references therein.
(37) Dunn, T. M. *Trans. Faraday Soc.* **1961**, *57*, 1441; *J. Chem. Soc. A* **1959**, 623.
(38) Martin, R. L.; White, A. H. *Nature* (*London*) **1969**, *53*, 601. Weiss, R.; Verkade, J. G. *Inorg. Chem.* **1979**, *18*, 529. Fujiwara, S.; Yajima, F.; Yamasaki, A. *J. Magn. Reson.* **1969**, *1*, 203.
(39) Bramley, R.; Brorson, M.; Sargeson, A. M.; Schäffer, C. *J. Am. Chem. Soc.* **1985**, *107*, 2780.
(40) Pidcock, A.; Richards, R. E.; Venanzi, L. M. *J. Chem. Soc. A* **1968**, 1970. Dean, R. R.; Green, J. C. *J. Chem. Soc. A* **1968**, 3047. Goggin, P. L.; Goodfellow, R. J.; Haddock, S. R.; Taylor, B. F.; Marshall, I. R. H. *J. Chem. Soc., Dalton Trans.* **1976**, 459.
(41) Becker, K. D.; Berlage, U. *J. Magn. Reson.* **1983**, *54*, 272.
(42) Kidd, R. G.; Truax, D. R. *J. Am. Chem. Soc.* **1968**, *90*, 6867. Schneider, W. G.; Buckingham, A. D. *Discuss. Faraday Soc.* **1962**, *34*, 147.
(43) Mason, J. *Chem. Rev.* **1981**, *81*, 205.
(44) Minelli, M.; Enemark, J. H.; Brownlee, R. T. C.; O'Connor, M. J.; Wedd, A. G. *Coord. Chem. Rev.* **1985**, *68*, 169.
(45) Freeman, R.; Murray, G. R.; Richards, R. E. *Proc. R. Soc. London, A* **1957**, *242*, 455.
(46) Brêvard, C.; Granger, P. *J. Am. Chem. Soc.* **1983**, *22*, 532.
(47) Mason, J.; Grieves, R. A. *Polyhedron* **1986**, *5*, 415.
(48) Looser, H.; Brinkmann, D. *J. Magn. Reson.* **1985**, *64*, 76.
(49) Christ, H. A.; Diehl, P.; Schneider, R. H.; Dahn, H. *Helv. Chim. Acta* **1961**, *44*, 865.
(50) Van Vleck, J. G. *Theory of Electric and Magnetic Susceptibilities*; Oxford University: Oxford, 1932; pp 275, 302.
(51) Figgis, B. N.; Kidd, R. G.; Nyholm, R. S. *Proc. R. Soc. London, A* **1962**, *269*, 469.
(52) Carrington, A. *Mol. Phys.* **1960**, *3*, 271. Carrington, A.; Schonland, D. S. *Ibid.* **1960**, *3*, 331. Carrington, A.; Jørgensen, C. K. *Ibid.* **1961**, *4*, 395.
(53) Orgel, L. E. *J. Chem. Soc.* **1958**, 4186; *Mol. Phys.* **1958**, *1*, 322.
(54) Koie, Y.; Shinoda, S.; Saito, Y. *J. Chem. Soc., Dalton Trans.* **1981**, 1082.
(55) Ballhausen, C. J. In *Molecular Electronic Structures of Transition Metal Complexes*; McGraw-Hill: New York, 1979; p 70.
(56) Maricq, M. M.; Waugh, J. S. *J. Chem. Phys.* **1979**, *70*, 3300. Herzfeld, J.; Berger, A. E. *J. Chem. Phys.* **1980**, *73*, 1021.
(57) Meadows, M. D.; Smith, K. A.; Kinsey, R. A.; Rothgeb, T. M.; Skarjune, R. P.; Oldfield, E. *Proc. Natl. Acad. Sci. U.S.A.* **1982**, *79*, 1351.
(58) Spiess, H. W.; Haas, H.; Hartmann, H. *J. Chem. Phys.* **1969**, *50*, 3057.
(59) Spiess, H. W.; Sheline, R. K. *J. Chem. Phys.* **1970**, *53*, 3036.
(60) Spiess, H. W.; Sheline, R. K. *J. Chem. Phys.* **1971**, *54*, 1099. Fenske, R. F.; DeKock, R. L. *Inorg. Chem.* **1970**, *9*, 1053. Evans, S.; Green, J. C.; Green, M. L. H.; Orchard, A. F.; Turner, D. W. *Discuss. Faraday Soc.* **1969**, *47*, 112.
(61) Mooberry, E. S.; Sheline, R. K. *J. Chem. Phys.* **1972**, *56*, 1852.
(62) Mooberry, E. S.; Spiess, H. W.; Sheline, R. K. *J. Chem. Phys.* **1972**, *57*, 813. Caulton, K. G.; Fenske, R. F. *Inorg. Chem.* **1968**, *7*, 1273.
(63) Slater, J. L.; Pupp, M.; Sheline, R. K. *J. Chem. Phys.* **1972**, *57*, 2105.
(64) Mooberry, E. S.; Pupp, M.; Slater, J. L.; Sheline, R. K. *J. Chem. Phys.* **1971**, *55*, 3655.
(65) (a) Keller, H. J.; Rupp, H. H. *Z. Naturforsch. A: Astrophys., Phys. Phys. Chem.* **1971**, *26A*, 785; **1970**, *25A*, 312. (b) Rupp, H. H. *Z. Naturforsch., A: Astrophys., Phys. Phys. Chem.* **1971**, *26A*, 1937. (c) Sparks, S. W.; Ellis, P. D. *J. Am. Chem. Soc.* **1986**, *108*, 3215. (d) Cotton, F. A.; Wilkinson, G. *Advanced Inorganic Chemistry*, 4th ed.; Wiley: New York, 1980; p 1110.
(66) Harris, R. K.; Reams, P.; Packer, K. J. *J. Chem. Soc., Dalton Trans.* **1986**, 1015.
(67) Honkonen, R. S.; Marchetti, P. S.; Ellis, P. D. *J. Am. Chem. Soc.* **1986**, *108*, 912.
(68) Jakobsen, H. J.; Ellis, P. D.; Inners, R. R.; Jensen, C. F. *J. Am. Chem. Soc.* **1982**, *104*, 7442.
(69) Mennitt, P. G.; Shatlock, M. P.; Bartuska, V. J.; Maciel, G. E. *J. Phys. Chem.* **1981**, *85*, 2087.
(70) Murphy, P. D.; Stevens, W. C.; Cheung, T. T. P.; Lacelle, S.; Gerstein, B. C.; Kurtz, D. M. *J. Am. Chem. Soc.* **1981**, *103*, 4400.
(71) Knight, C. T. G.; Turner, G. L.; Kirkpatrick, R. J.; Oldfield, E. *J. Am. Chem. Soc.* **1986**, *108*, 7426.
(72) Kazanskii, L. P. *Bull. Acad. Sci. USSR., Div. Chem. Sci.* (*Engl. Transl.*) **1975**, 429. Kazanskii, L. P.; Torchenkova, E. A.; Spitsyn, V. I. *Dokl. Akad. Nauk SSSR* **1973**, *213*, 118.
(73) Jenny, T.; Von Philipsborn, W.; Kronenbitter, J.; Schwenk, A. *J. Organomet. Chem.* **1981**, *205*, 211.
(74) Koridze, A. A.; Astakhova, N. M.; Petrovskii, P. V. *J. Organomet. Chem.* **1983**, *254*, 345.
(75) Green, J. C.; Grieves, R. A.; Mason, J. *J. Chem. Soc., Dalton Trans.* **1986**, 1313, and unpublished observations.
(76) Mason, J., to be submitted for publication.
(77) Akitt, J. W.; McDonald, W. S. *J. Magn. Reson.* **1984**, *58*, 401.
(78) Pyykkö, P.; Desclaux, J.-P. *Acc. Chem. Res.* **1979**, *12*, 276. Pitzer, K. S. *Ibid. 271*; McKelvey, D. R. *J. Chem. Educ.* **1983**, *60*, 112.
(79) Pyykkö, P. *Chem. Phys.* **1983**, *74*, 1. Pyper, N. C. *Chem. Phys. Lett.* **1983**, *96*, 204.
(80) Slichter, C. P. *Principles of Magnetic Resonance*; Springer-Verlag: Berlin, 1978; p 134.
(81) Nomura, Y.; Takeuchi, Y.; Nakagawa, N. *Tetrahedron Lett.* **1969**, *639*; Morishima, I.; Mizuno, A.; Yonezawa, T. *Chem. Phys. Lett.* **1970**, *78* 633.
(82) Morishima, I.; Endo, K.; Yonezawa, T. *J. Chem. Phys.* **1973**, *59*, 3356; Volodicheva, M. I.; Rebane, T. K. *Theor. Exp. Chem.* (*Engl. Transl.*) **1978**, *14*, 348.
(83) Cheremisin, A. A.; Schastnev, P. V. *J. Magn. Reson.* **1980**, *40*, 459.
(84) Tripathi, G. S.; Misra, C. M.; Misra, P. K. *J. Phys. C* **1985**, *18*, L935.
(85) In this paper the periodic group notation is in accord with recent actions by IUPAC and ACS nomenclature committees. A and B notation is eliminated because of wide confusion. Groups IA and IIA become groups 1 and 2. The d-transition elements comprise groups 3 through 12, and the p-block elements comprise groups 13 through 18. (Note that the former Roman number designation is preserved in the last digit of the new numbering: e.g., III → 3 and 13.)